

## Research on optimization method of flotation kinetic model based on molybdenite particle size effect

He Wan <sup>1</sup>, Yanni An <sup>1</sup>, Juanping Qu <sup>2</sup>, Chonghui Zhang <sup>1</sup>, Jiwei Xue <sup>1</sup>, Sen Wang <sup>1</sup>, Xianzhong Bu <sup>1</sup>

<sup>1</sup> School of Resource Engineering, Xi'an University of Architecture and Technology, Xi'an 710055, China

<sup>2</sup> Oulu Ming School, University of Oulu, Oulu, F1-90014, Finland

Corresponding authors: wanhe@xauat.edu.cn (He Wan), buxianzhong@xauat.edu.cn (Xianzhong Bu)

**Abstract:** Flotation kinetic models can be applied to describe the flotation process and to predict mineral recoveries. However, the size composition of the target minerals in the feed ore fluctuates considerably, resulting in insufficient accuracy with flotation kinetic models. There have been many studies that focus on the investigation of flotation kinetics with different particle sizes, while the optimization methods for flotation kinetic models based on particle size effects have not been reported. In this paper, flotation tests, optical microscope observations, and particle size analysis were used to identify the reasons for the decrease in accuracy of the flotation kinetic model due to changes in the composition of molybdenite particle size. Additionally, an optimization method for the flotation kinetic model was developed based on the particle size effect. The test results show that the accuracy of the flotation kinetic model for fixed particle size minerals is very high, but the predicted results for flotation recoveries of different particle size mineral mixtures have large deviations. The poor accuracy might be due to the autogenous carrier effect caused by the particle size composition fluctuating considerably. The optimization method for the flotation kinetic model is based on the particle size effect. The model can accurately describe the flotation process of molybdenite with different size compositions of molybdenite and predict the flotation recovery of molybdenite.

**Keywords:** particle size effect, molybdenite, mathematical model, method of correction

### 1. Introduction

Mineral resources have been exploited in large quantities, especially those readily available minerals that have gradually reduced. In addition, the mineral particle size composition is becoming finer, and the properties are becoming more complex, which brings severe challenges to the mineral processing industry (Zhang et al., 2013). Flotation is the most widely used and effective beneficiation method for separating fine refractory minerals (Ni et al., 2016). However, flotation is a complex physical and chemical process influenced by many factors, including the properties of the ore itself, flotation equipment parameters, and reagents (Xu et al., 2012; Polat et al., 2003; Feng et al., 2022; Jovica et al., 2018; Zhang et al., 2019). The flotation kinetics is an essential aspect of the study of the flotation process. The flotation kinetics model can describe the flotation process, which relates different process parameters such as particles and pulp with a flotation rate constant. Therefore, establishing a flotation kinetic model is essential in optimizing process parameters, improving flotation flow, automating beneficiation production, and predicting the flotation index (Gharai et al., 2016). Particle size has a crucial effect on the flotation rate and is one of the most critical parameters in the flotation process (Cheng et al., 2013; Rahman et al., 2012; Huang et al., 2018).

Many scholars have researched the influence of particle size on flotation kinetics. Luo et al. studied the flotation kinetics of coal slime with different particle sizes to investigate the influence of coal slime particle size on its flotation kinetic (Luo et al., 2015). Abkhoshk et al. researched the effects of density and particle size on the flotation rate constant ( $k$ ) (Abkhoshk et al., 2010). They predicted the production results of the modified continuous flotation kinetic model. Luo et al. proposed the optimal

flotation kinetics model suitable for different particle sizes of slime by analyzing the flotation rates of narrow and different particle-size mineral mixtures of coal (Luo et al., 2015). On this basis, Yang et al. used Excel software to establish the mathematical model of the flotation yield, ash content, and flotation time of the refined coal of each particle grade. Combined with the particle size composition, the different particle size mineral mixtures flotation mathematical model was derived, which had high reliability and could accurately predict the technical flotation indicators (Yang et al., 2020). However, the size composition of the target minerals in the feed ore fluctuates considerably, resulting in insufficient accuracy with flotation kinetic models. This is a unified problem after research by many scholars. But the flotation mathematical model of different particle size compositions has yet to be reported.

To address this problem, this paper investigates the effect of the particle size composition of molybdenite on its flotation kinetic model and identifies the reasons for the decrease in accuracy of the flotation kinetic model due to changes in the particle size composition of molybdenite. And develops an optimization method for the flotation kinetic model based on the particle size effect, establishing a flotation kinetic model for molybdenite that is not affected by the particle size effect. The model can accurately describe the flotation process of molybdenite with different size compositions and predict the flotation recovery of molybdenite. Moreover, this work could provide a theoretical basis for the development of flotation kinetic models for complex and variable conditions.

## 2. Materials and methods

### 2.1. Materials

The molybdenite (primary concentrate) was obtained from Jinduicheng Molybdenum Group Co., Ltd located in Shaanxi Province, China. By the provisions of the national standard, the test ore samples were wet screened by 148 $\mu$ m, 75 $\mu$ m, 45 $\mu$ m, and 38 $\mu$ m standard screens, respectively. Representative flotation feed samples of various sizes were prepared by the conical quartering method and stored in sealed plastic bags to avoid oxidation. The screening test results are shown in Table 1.

Table 1. Flotation feed screening analysis

Particle range ( $\mu$ m)	Individual yield (%)	Cumulative yield (%)	Grade of Mo (%)	The distribution rate of Mo (%)
+148	10.56	10.56	5.56	4.62
-148+75	10.98	21.54	10.63	9.17
-75+45	13.94	35.48	22.48	24.53
-45+38	9.08	44.56	38.42	27.35
-38	55.44	100	7.90	34.33
Total	100		12.76	100

As shown in Table 1, the yield of coarse particles (+75 $\mu$ m), medium particles (-75+38 $\mu$ m), and fine particles (-38 $\mu$ m) were 21.54%, 23.02%, and 55.44%, respectively. The fine particles in the flotation feed are the dominant particle size, and their separation is the key to the whole flotation process. Generally, the floatability of medium particle size is better than coarse and fine particles; however, it can be seen from Table 1 that the total yield of coarse and fine particles is 76.98%, which leads to the difficulty of molybdenite recovery. From the Mo grade, the coarse, medium, and fine particles are 13.79%, 51.88%, and 34.33%, respectively. More than half of Mo is distributed in the medium fraction, which is conducive to flotation recovery.

### 2.2. Flotation experiments

Flotation experiments were performed with a flotation cell (XFD 0.5L) at a rotating speed of 2000r/min. The flotation temperature is 25°C (room temperature). During the flotation process, 80.0g molybdenite was mixed with 0.5L of deionized (DI) water in the flotation cell for 2min. The duration of the flotation process was 4min. Eight flotation concentrate products (RC1, RC2, RC3, RC4, RC5, RC6, RC7, and RC8) were collected after 0.5min, 1.0min, 1.5min, 2.0min, 2.5min, 3min, 3.5min and 4min, respectively. Finally, the concentrates and tailings were collected, filtered, dried, and weighed

after flotation, respectively. The results of the grade are used to calculate the flotation recovery. Each flotation experiment was repeated at least thrice times, and the mean values was recorded. The flotation flowsheet is presented in Fig. 1.

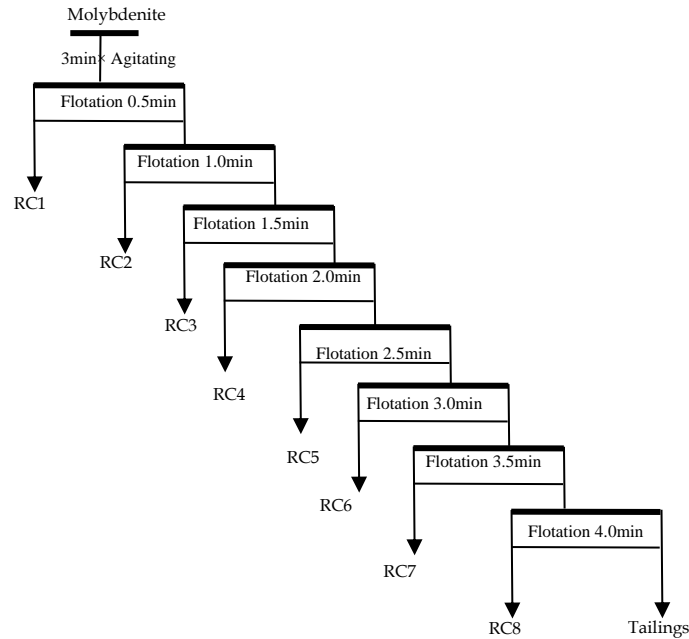


Fig. 1. Flow diagram of flotation experiments

### 2.3. Flotation kinetics model

HSC Chemistry software contains modules for mineral processing and particle calculation, integrated with a wide range of mineral databases. The flotation kinetics of the flotation rate law of molybdenite of each size fraction and different particle-size mineral mixtures was studied. Table 2 shows the four flotation kinetic models fitted by HSC Chemistry analysis software for the cumulative recoveries collected in the flotation test.

Table 2. Flotation equations in HSC sim model fit

Model	Lab equation (batch)	Constraints
One-component	$R = (1 - \exp(-kt))$	
Two-component	$R = m_F (1 - \exp(-k_F t)) + m_S (1 - \exp(-k_S t))$	$m_F + m_S = 1$ $k_F \geq k_S$
Three-component	$R = m_F (1 - \exp(-k_F t)) + m_S (1 - \exp(-k_S t)) + m_N$	$m_F + m_S + m_N = 1$ $k_F \geq k_S$
Rectangular Distribution	$R = \left(\frac{R_\infty}{b}\right) \sum_{i=1}^b (1 - \exp(-k_i t))$ $k_i = \frac{k_{max}}{b}$ $k_{i>1} = k_{i-1} + k_1$	$R_\infty \leq 1$ $b = 15$

The  $k$  corresponds to the first-order rate constant ( $\text{min}^{-1}$ ), and  $t$  represents the flotation time (min) in the One-component model expression. In the two-component model expression,  $m_F$ - maximum recovery of fast flotation minerals (%),  $m_S$ - maximum recovery rate of slow floating mineral (%),  $k_F$ - flotation rate constant of fast-floating minerals ( $\text{min}^{-1}$ ),  $k_S$ - flotation rate constant of slow-floating minerals ( $\text{min}^{-1}$ ). In the three-component model expression,  $m_N$ -maximum recovery rate of non-floating minerals (%). The flotation rate constant of non-floating minerals is 0. In the rectangular distribution model expression,  $R_\infty$ - maximum recovery (%),  $k_{Max}$ - Maximum flotation rate constant ( $\text{min}^{-1}$ ).

## 2.4. Optical microscopy analysis

2.0g of molybdenite was mixed with 40mL DI water in a beaker was stirred in a constant temperature mechanical equipment magnetically for 3min. Subsequently, remove 2mL pulp with a syringe and transfer to a beaker diluted five times with DI water. After stirring, the diluted solution was dropped on a glass slide for optical microscope observation.

## 2.5. Particle size measurements

The particle size distribution of the sample was measured by Mastersizer 2000 laser particle size analyzer. The sample is prepared similarly to the flotation test. Then, filtered and dried for the particle size measurement. During the measurements, lightly stir the sample to keep the particles suspended in the slurry. Subsequently, 1ml of pulp was extracted from the suspension for the measure. Repeat each measurement at least three times.

## 3. Results and discussion

### 3.1. Flotation test of molybdenite with different sizes and different particle size mineral mixtures

The cumulative recovery as a function of the flotation time for different sizes and different particle-size mineral mixtures is presented in Fig. 2.

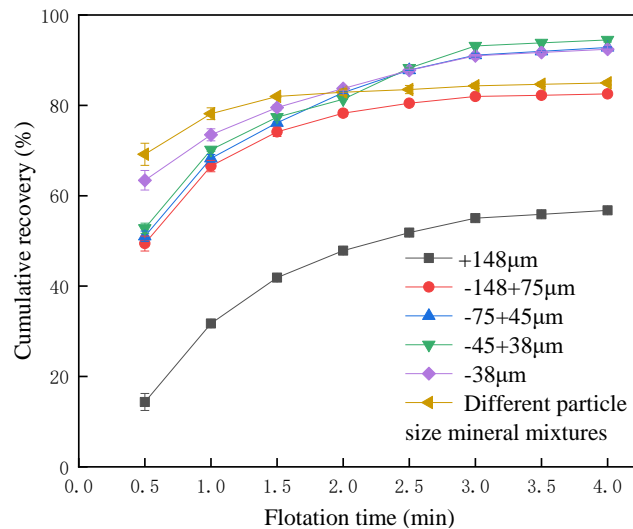


Fig. 2. Effect of particle size on the cumulative recovery

As is evident from Fig. 2 that the cumulative flotation recovery of molybdenite of each particle size will increase with the flotation time. However, under the same test conditions, the floatability of molybdenite with different particle sizes has light differences. Medium-sized molybdenite has good floatability, while the floatability of coarse molybdenite is reduced. The flotation rate of coarse particles is slow due to their large mass, high desorption probability, and slightly poor hydrophobicity of the intergrowth. The flotation rate of fine particles is faster than coarse particles because of their small mass and volume, high adhesion probability with bubbles, and small desorption probability. The cumulative recovery rate of -148+75µm is close to the medium particle size, which may be that the molybdenite in the body of the coarser particles aggregate is in the form of scales, felts, and irregular aggregates (Yuan et al., 2010); therefore, realizing the dissociation of molybdenite scales and gangue is easier under this particle size. The high dissociation of monomers led to a significant increase in grade, and the fine particles entrainment led to a higher yield, which ultimately led to -38µm having a higher cumulative recovery (Liu et al., 2008). The cumulative flotation recovery of the different particle size mineral mixtures is higher than the other particle fractions before 2min, while the growth is slow and stable in the last 2min. This phenomenon is because the coarse and some fine particle concentrates

slowly emerge. Some fine particle concentrates have large specific surface areas and significant content of fine mud, so they can only emerge after a long time of mineralization.

### 3.2. Flotation kinetics of molybdenite with classification and component velocity

Molybdenite with different sizes and different particle size mineral mixtures were used to study the effect of grain size on flotation kinetics. Kinetic tests of molybdenite with different particle sizes were carried out by HSC Chemistry analysis software. The correlation coefficient ( $R^2$ ) is one of the criteria used to judge the accuracy of flotation kinetic models, which is widely used in evaluating and comparing with flotation models. The larger the value of  $R^2$ , the better the model's fit. The larger the value of the flotation rate constant ( $k$ ), the faster the flotation rate.

Fig. 3 shows the fitting results of the four kinetic models and the test data. According to the fitting between the four kinetic models and the experimental data in Fig. 3, the fitting effect of model 1 ( $R^2=0.915$ ) with +148 $\mu\text{m}$  was the worst, and Model 4 ( $R^2=0.988$ ) was better than model 1. Model 2 and model 3 had the best fitting effect ( $R^2=0.991$ ). The kinetic parameters of Model 3 include the maximum recovery rate of non-floating minerals, which can more accurately reflect the flotation behavior of practice minerals. Therefore, it can best describe the influence of particle size (+148 $\mu\text{m}$ ) on flotation kinetics. For the particle size of -148+75 $\mu\text{m}$ , the fitting effect of model 2 is as good as model 3, and the  $R^2$  value is the largest (0.999). Model 1 had the worst effect ( $R^2=0.962$ ). Model 4 ( $R^2=0.997$ ) was better than model 1.

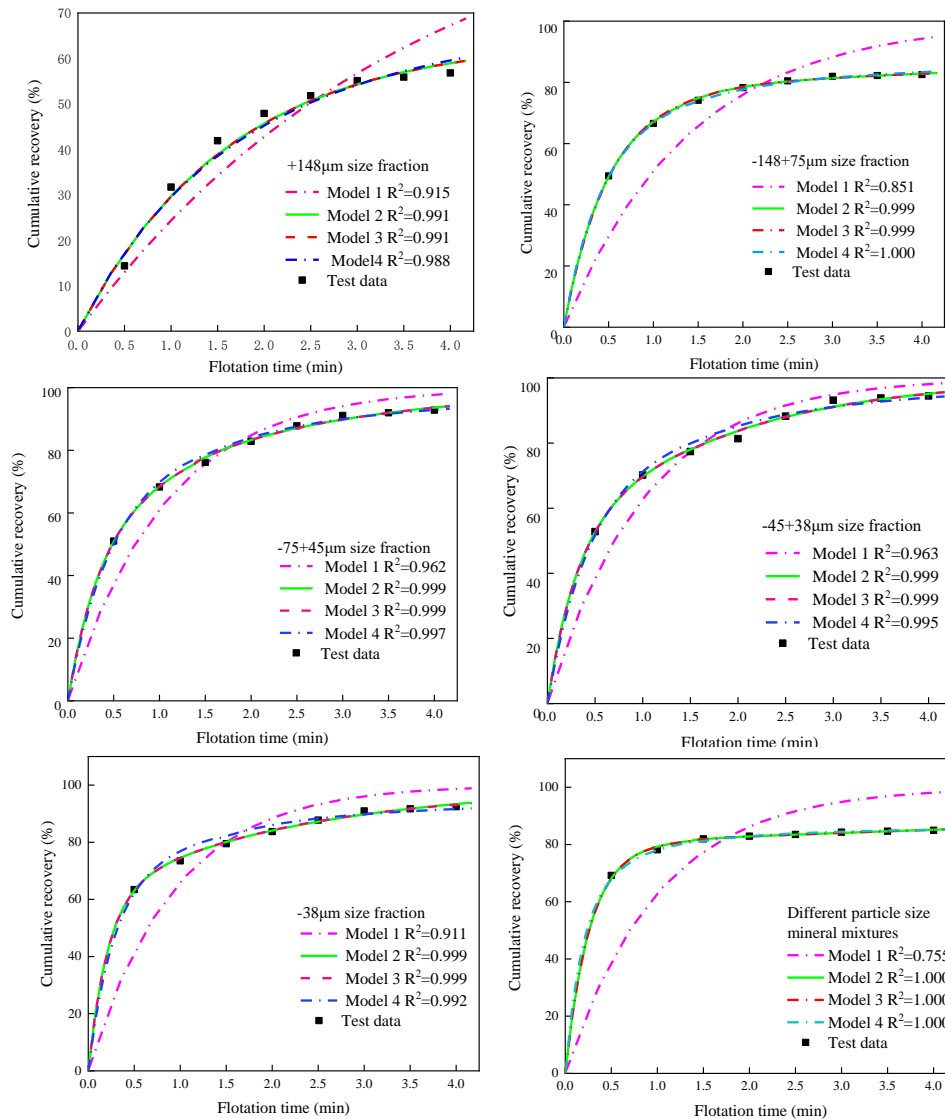


Fig. 3. The kinetic models fitted to test data of flotation

For -75+45 $\mu\text{m}$  particle size, the  $R^2$  value for model 2 and model 3 that fitted the flotation results was 0.999, which is the best. The second is model 4 ( $R^2=0.997$ ), and the worst effect is model 1 ( $R^2=0.962$ ). For -45+38 $\mu\text{m}$  particle size, the  $R^2$  value for model 2 and model 3 that fitted the flotation results was 0.999, which is the best. The second is model 4 ( $R^2=0.995$ ), and the worst effect is model 1 ( $R^2=0.963$ ). For -38 $\mu\text{m}$  particle size, the  $R^2$  value for model 2 and model 3 that fitted the flotation results was 0.999. It is relatively consistent with the actual flotation test results, which can accurately predict the maximum recovery rate of actual flotation to a large extent. The second is model 4 ( $R^2=0.992$ ), and the worst effect is model 1 ( $R^2=0.911$ ). For the different particle size mineral mixtures, the  $R^2$  value for models 2, 3, and 4 that fitted the flotation results was 1.000, with a particular reference value. The relevant results are consistent with the actual flotation test results and can accurately predict the maximum recovery rate of actual flotation to a large extent. The worst effect was model 1 ( $R^2=0.755$ ).

To compare the flotation kinetic models of molybdenite of each particle size and different particle size mineral mixtures, deeply explore the influence of particle size on flotation kinetics, and systematically analyze the fitting parameters of the four kinetic models, as indicated in Table 3. The kinetic parameter of model 1 is the flotation rate constant ( $k$ ). Model 2 includes fast-floating components and slow-floating components. The kinetic parameters are fast floating mineral rate constant ( $k_F$ ) and slow floating mineral rate constant ( $k_s$ ), and the maximum recovery rate of fast-floating minerals ( $m_F$ ) and slow-floating minerals ( $m_s$ ). Model 3 divides each mineral into fast, slow, and non-floating components. The kinetic parameters are more than model 2 in terms of maximum recovery of non-floating minerals ( $m_N$ ). This mathematical model is flexible. The kinetic parameters of model 4 include the maximum recovery ( $R_{inf}$ ) and the maximum flotation velocity constant ( $k_{Max}$ ).

Table 3. Fitting parameters of flotation kinetic model

Number	Parameter	1	2	3	4	5	6
	s						
Size distribution/ $\mu\text{m}$		+148	-148+75	-75+45	-45+38	-38	Different particle-size mineral mixtures
Model 1	$k$ ( $\text{min}^{-1}$ )	0.279	0.716	0.947	0.993	1.081	0.994
	$m_F$ (%)	64.3	77.5	59.4	45.8	62.0	80.2
Model 2	$m_s$ (%)	35.7	22.5	40.6	54.2	38.0	19.8
	$k_F$ ( $\text{min}^{-1}$ )	0.62	1.87	2.312	3.60	4.274	3.653
	$k_s$ ( $\text{min}^{-1}$ )	0.00	0.069	0.464	0.604	0.437	0.072
	$m_F$ (%)	64.3	77.2	59.6	45.8	59.6	80.0
	$m_s$ (%)	19.4	13.8	40.4	54.2	38.6	14.2
Model 3	$m_N$ (%)	16.2	9.0	0.00	0.00	1.8	5.8
	$k_F$ ( $\text{min}^{-1}$ )	0.62	1.873	2.303	3.597	4.569	3.677
	$k_s$ ( $\text{min}^{-1}$ )	0.00	0.133	0.463	0.605	0.508	0.113
Model 4	$R_{inf}$ (%)	75.60	86.79	99.044	100	94.84	85.902
	$k_{Max}$ ( $\text{min}^{-1}$ )	1.01	3.71	2.740	2.796	4.076	8.072

The fitting results of the kinetic model and flotation data in Fig. 3 show that the fitting effect of each particle fraction and the different particle size mineral mixtures model 3 is the best. It can be seen from model 3 that the maximum recovery rate of fast-floating minerals of all particle sizes and different particle-size mineral mixtures are dominant. Therefore, the kinetic parameters of model 3 are mainly analyzed, including the maximum recovery rate of fast-floating minerals ( $m_F$ ), the maximum recovery rate of non-floating minerals ( $m_N$ ), and the rate constant of fast-floating minerals ( $k_F$ ). The particle size distribution significantly affects the cumulative recovery of molybdenite. The  $m_F$  in each particle size fraction and different particle size mineral mixtures are arranged from large to small as follows: different particle size mineral mixtures (80.0%), -148+75 $\mu\text{m}$  (77.2%), +148 $\mu\text{m}$  (64.3%), -38 $\mu\text{m}$  (59.6%), -75+45 $\mu\text{m}$  (59.6%), -45+38 $\mu\text{m}$  (45.8%). In addition, the maximum recovery rate of non-floating

minerals ( $m_N$ ) for +148 $\mu\text{m}$  size particles, -148+75 $\mu\text{m}$  and -38 $\mu\text{m}$  are 16.2%, 9% and 1.8% respectively. The maximum recovery rate of actual flotation can be accurately predicted to a large extent. At the same time, it is different from the change of the flotation rate constant.

The change in the  $k$  value reflects the influence of particle size distribution on the variation law of the molybdenite flotation rate. The  $k_F$  of each particle size fraction and different particle size mineral mixtures from large to small is as follows: -38 $\mu\text{m}$  (4.569 $\text{min}^{-1}$ ), the different particle size mineral mixtures (3.677 $\text{min}^{-1}$ ), -45+38 $\mu\text{m}$  (3.597 $\text{min}^{-1}$ ), -75+45 $\mu\text{m}$  (2.303 $\text{min}^{-1}$ ), -148+75 $\mu\text{m}$  (1.873 $\text{min}^{-1}$ ), +148 $\mu\text{m}$  (0.62 $\text{min}^{-1}$ ). The particle size of +148 $\mu\text{m}$  is large, and the desorption probability is high. Therefore, the flotation rate constant is low (Huang et al., 2013). It is not easy to reach the flotation balance and needs a longer mineralization time to achieve. However, the flotation constant of -148+75 $\mu\text{m}$  fast-floating minerals is relatively large, which is easier to reach the flotation equilibrium. With the decrease in particle size, the flotation constants of fast-floating minerals of -75+45 $\mu\text{m}$  and -45+38 $\mu\text{m}$  gradually increase.

Moreover, the difference between the flotation velocity coefficients of these two particle sizes is slight, and their change rules of them are similar. The main reason is that the particle size of this part is moderate, which is conducive to the adhesion of particles, and the probability of falling off is small (Luo et al., 2015). The flotation constant of different particle size mineral mixtures of fast-floating minerals is higher than that of the above four particle stages, which may be due to the collision and carrying between coarse particles and fine particles in the flotation process, which will play a key role in promoting the flotation of fine particles. The flotation constant of fast-floating minerals for -38 $\mu\text{m}$  is higher, which is inconsistent with the flotation rate of fine particles in general. The reason may be that the -38 $\mu\text{m}$  has a good monomer dissociation degree, or the foam adhered to some particles on the surface of the flotation tank, which quickly surfaced and reached flotation equilibrium at the beginning of flotation; therefore, the flotation rate is relatively high in a short time.

### 3.3. Mathematical model of molybdenite with classification and fractional velocity

#### 3.3.1. Establishment of the mathematical model for molybdenite with classification and fractional velocity

The existing flotation kinetics model cannot predict the flotation process of complex particle size composition by the method in the form of summation for multiple particle sizes. We fit the flotation data and derive its polynomial equation to solve this problem. The equation can be used to describe the flotation process of complex particle size composition in the form of summation of different particle size compositions; at the same time, the optimized polynomial-fitted flotation kinetics equation is suitable for the prediction of flotation indexes of molybdenum ore with various particle size compositions.

Excel deduces the flotation rate equation of each particle size. That is, the trend line is added to the curve of each particle size. The prediction type of trend line is polynomial, the number of items is set as 3, and the formula and the fair value of fitting precision value  $R^2$  are displayed. The multivariate nonlinear models of cumulative recovery ( $y$ ) and flotation time ( $t$ ) of each particle size are established as follows:

$$y = A_1 t^3 + B_1 t^2 + C_1 t + D_1$$

Through calculation and fitting of flotation rate test data of each particle size, the correlation coefficient of the flotation mathematical model of each particle size is indicated in Table 4.

Table 4. Relevant parameters of flotation mathematical model of each particle size

Particle size ( $\mu\text{m}$ )	$A_1$	$B_1$	$C_1$	$D_1$	$R^2$
+148	1.451	-14.653	51.511	-7.463	0.998
-148 +75	1.863	-17.091	52.293	28.014	0.995
-75 +45	1.094	-11.862	45.190	32.015	0.996
-45+38	0.855	-9.701	39.730	36.550	0.987
-38	0.397	-5.369	25.118	52.534	0.997

Table 4 shows that the fitting  $R^2$  of the derived mathematical model for flotation of each particle fraction is close to 1, with a high degree of fitting, indicating that the model has high accuracy. Combined with Table 1, the particle size coefficients of each particle size fraction are determined to be 0.11, 0.11, 0.14, 0.09, and 0.55, respectively. Multiplying them by the derivation model of the corresponding particle size, we can get the multivariate nonlinear model of the cumulative recovery ( $y$ ) and flotation time ( $t$ ) of different particle size mineral mixtures molybdenite as follows:

$$y = 0.813t^3 - 8.978t^2 + 35.136t + 38.925$$

The predicted results of the derived different particle size mineral mixtures model are compared with the laboratory's actual different particle size mineral mixtures flotation rate test results to verify the reliability of the derived mathematical model of different particle size mineral mixtures flotation, as demonstrated in Fig. 4. It can be seen from Fig. 4 that the coincidence degree of the two curves is poor. Its internal mechanism needs to be further explored.

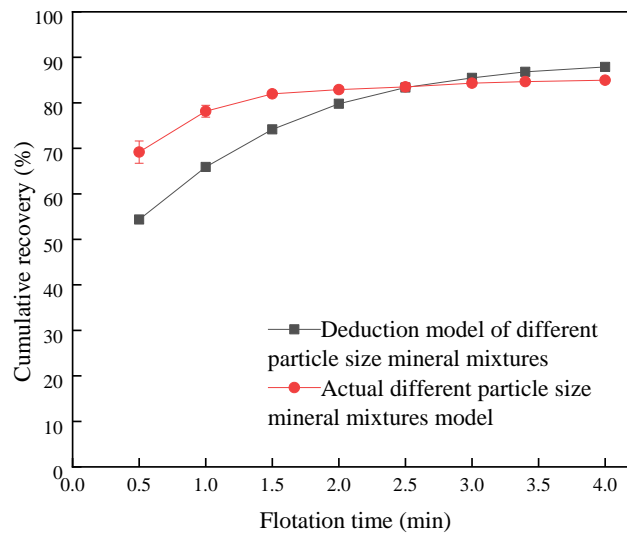


Fig. 4. Derivation of different particle size mineral mixtures model and results of actual different particle size mineral mixtures flotation rate test

### 3.3.2. Inherent reasons for differences in mathematical models of molybdenite with classification and fractional velocity

Optical microscope analysis is widely used to determine mineral particles' dispersion and agglomeration performance in the pulp (Li et al., 2017; Liu et al., 2014). Therefore, the pure molybdenite mineral is used as the research object to study the performance of the pulp under different conditions. The results are presented in Fig. 5.

As is evident from Fig. 5 (a) those fine particles  $-38\mu\text{m}$  exist in the pulp in a dispersed state. As shown in Fig. 5 (b),  $-148+75\mu\text{m}$  coarse particles also exist in the pulp in a dispersed state. However, it can be seen from Fig. 5 (c) and (d) that when  $-148+75$  and  $-38\mu\text{m}$  exist simultaneously, the fine particles will agglomerate on the surface of the coarse particles, consistent with the flotation result. The fine particles adhere to the coarse particles carrier, bearing the burden of fine particles floating up, improving the flotation effect of fine particles, and reflecting the self-carrier impact of molybdenite flotation.

The change in particle size can also reflect the dispersion and agglomeration behavior of ore sample particles in the pulp. Therefore, the particle size of molybdenite under different conditions is analyzed, and the results are shown in Fig. 6.

Under the vigorous agitation of the flotation cell, the collision probability between fine particles and coarse particles is far greater than the agglomeration rate between fine particles, which can make fine particles adhere to coarse particles (Zhang et al., 2017; Bu et al., 2017; Wang et al., 2020; Li et al., 2017; Xu et al., 2013). When the coarse and fine particles exist simultaneously, the fine particles will agglomerate on the surface of the coarse particles, as shown in Fig.7 (c) and (d), thus improving the



flotation effect of the fine particles. However, under the action of a turbulent shear field, the fine aggregates attached to the coarse grains will desorb and become intermediates due to shearing and grinding (Qiu et al., 1994). As shown in Fig. 6, a large number of intermediate particles between +38 $\mu\text{m}$  and coarse particles were generated after the coarse-grained carrier was added.

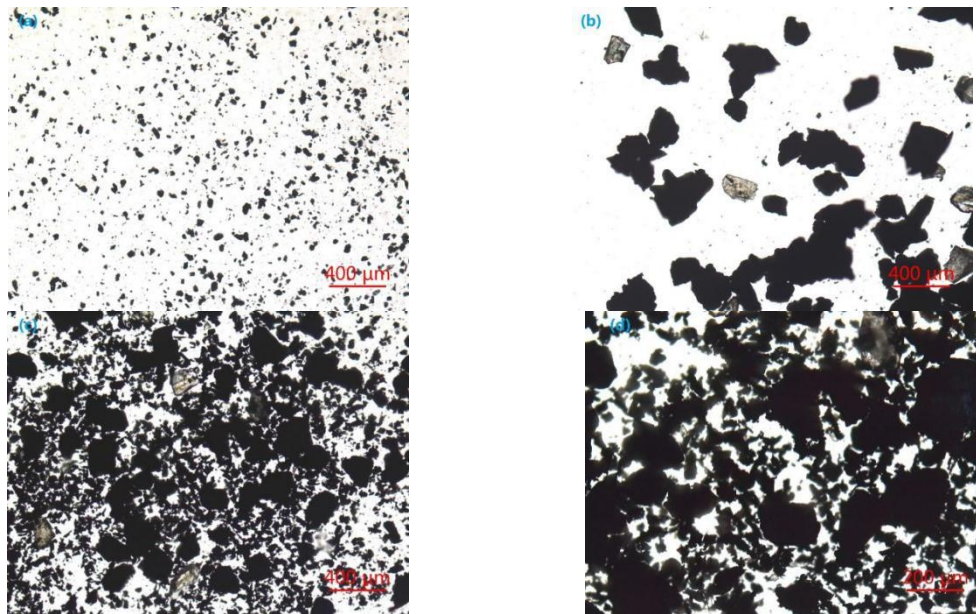


Fig. 5. Optical microscope observation of molybdenite particles (a: -38 $\mu\text{m}$ ; b: -148+75 $\mu\text{m}$ ; c, d: -148+75 $\mu\text{m}$  and -38 $\mu\text{m}$ )

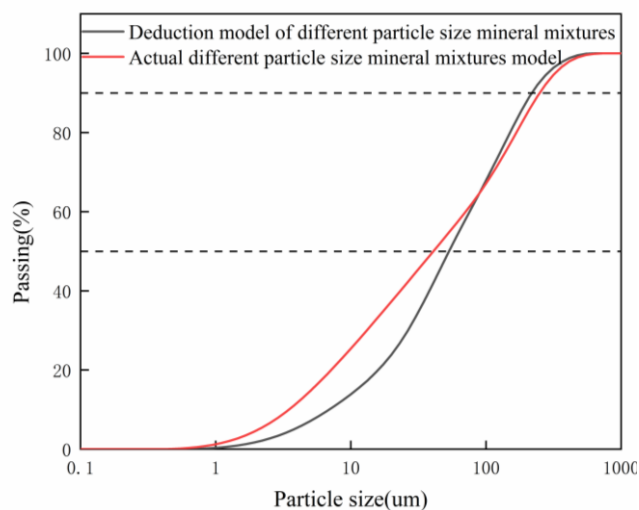


Fig. 6. Cumulative particle size distribution under different conditions (model-derived different particle size mineral mixtures and laboratory actual different particle size mineral mixtures)

### 3.3.3. Revision of flotation mathematical model based on carrier effect

Correction coefficient refers to the coefficient added to the calculation formula to make it reflect the actual performance as much as possible when there is a deviation between ideal and reality, reality, and investigation in data calculation and formula expression, generally expressed by  $\alpha$ . This paper uses four ore blending schemes to determine the correction coefficient, improve the reliability of the different particle size mineral mixtures flotation mathematical model, and make it possible to predict the flotation results. The proportion of -38 $\mu\text{m}$  is 55% unchanged, and the ratio of other particles is 45%, respectively.

Excel can derive the flotation rate equation of each scheme from the results of the flotation test of ore blending in the laboratory. That is, the trend line is added to the curves of each scheme. The correlation coefficients of each ore blending scheme were obtained through the calculation and fitting of the flotation rate test data of each ore blending scheme's actual flotation mathematical models, as indicated in Table 5.

Table 5. Relevant parameters of the actual flotation mathematical model of each ore blending scheme

Scheme	Particle size ( $\mu\text{m}$ )	$A_1$	$B_1$	$C_1$	$D_1$	$R^2$
Scheme 1	+148 with -38	1.325	-11.527	34.329	29.954	0.990
Scheme 2	-148+75 with -38	1.411	-12.589	37.244	51.773	0.997
Scheme 3	-75+45 with -38	1.653	-14.091	38.807	57.749	0.983
Scheme 4	-45+38 with -38	2.015	-17.114	47.676	51.213	0.976

As can be seen from Table 5, the fitting  $R^2$  of the actual flotation mathematical model of each ore blending scheme is close to 1, with a high suitable degree, indicating high accuracy. Table 6 shows the derived model multiplied by the particle size coefficient of 0.45 and 0.55 to obtain the flotation mathematical model of ore blending.

Table 6. The mathematical flotation models result derived from ore blending schemes.

Scheme	Particle size ( $\mu\text{m}$ )	Proportion	Multivariate nonlinear model
Scheme 1	+148 with -38	+148 $\mu\text{m}$ (45%)、-38 $\mu\text{m}$ (55%)	$y = 0.871t^3 - 9.546t^2 + 36.994t + 25.535$
Scheme 2	-148+75 with -38	-148+75 $\mu\text{m}$ (45%)、-38 $\mu\text{m}$ (55%)	$y = 1.057t^3 - 10.644t^2 + 37.346t + 41.500$
Scheme 3	-75+45 with -38	-75+45 $\mu\text{m}$ (45%)、-38 $\mu\text{m}$ (55%)	$y = 0.711t^3 - 8.291t^2 + 34.150t + 43.300$
Scheme 4	-45+38 with -38	-45+38 $\mu\text{m}$ (45%)、-38 $\mu\text{m}$ (55%)	$y = 0.603t^3 - 7.318t^2 + 31.693t + 45.341$

Fig. 7 compares the actual ore blending model and the derived ore blending model. Combined with Tables 5 and 6, it can be seen that there are differences in the coefficients between the actual ore blending model and the derived model, and the coincidence of the recovery rate is poor. Therefore, the actual ore blending model and the derived model coefficient were systematically analyzed to determine the correction coefficient.

### 3.3.4. Optimization of fractional flotation mathematical model for molybdenite

The coefficient ratio between the actual ore blending model and the derived model reflects the carrier effect of coarse particles on fine particles. Table 7 shows the analysis results of various coefficients of the actual ore blending model and the derived ore blending model.

Table 7. Analysis results of coefficients of the actual ore blending model and the derived ore blending model

Particle size ( $\mu\text{m}$ )	$A_1$	$B_1$	$C_1$	$D_1$
+148 with -38	1.520	1.212	0.927	1.173
-148+75 with -38	1.335	1.182	0.997	1.247
-75+45 with -38	2.324	1.699	1.136	1.333
-45+38 with -38	3.340	2.388	1.504	1.129

The coefficients of coarse particles are 0.244, 0.244, 0.312, and 0.2, respectively, which can be multiplied by the coefficient ratio of the corresponding coarse particles to obtain their correction coefficients. Therefore, the correction coefficients of coarse particles are 2.09 ( $\alpha_1$ ), 1.58 ( $\alpha_2$ ), 1.12 ( $\alpha_3$ ), and 1.23 ( $\alpha_4$ ), respectively. Therefore, the different particle size mineral mixtures flotation mathematical model optimized based on the carrier effect is  $y = 1.699t^3 - 14.195t^2 + 39.533t + 47.974$ . The reliability of the optimized different particle size mineral mixtures flotation

mathematical model is verified by comparing it with the actual different particle size mineral mixtures flotation test results in the laboratory (Fig. 8).

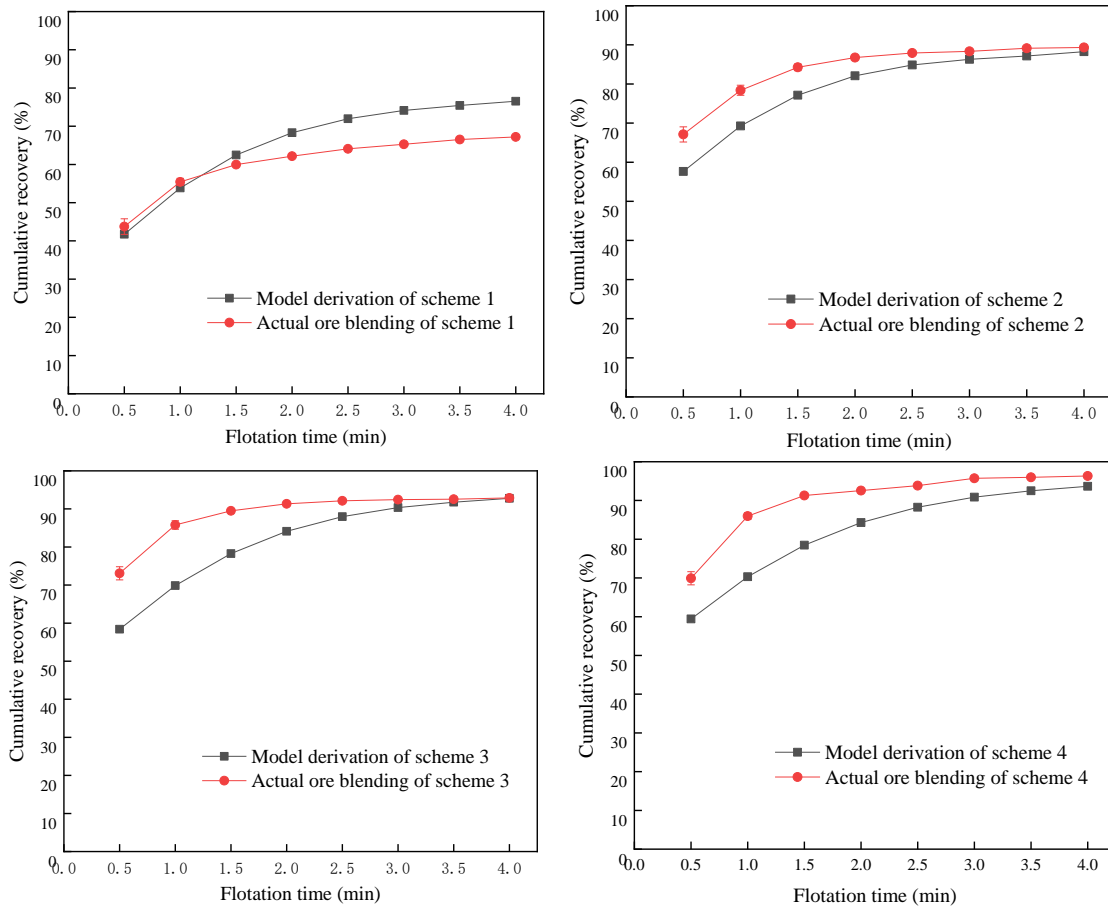


Fig. 7. Comparison between the actual ore blending model and derived ore blending model

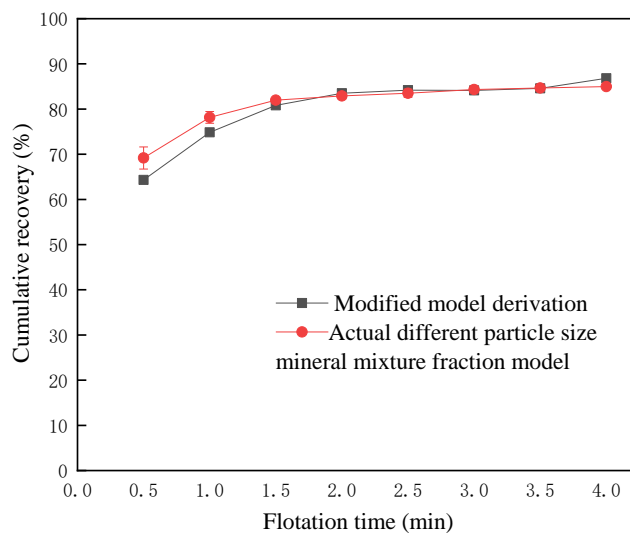


Fig. 8. Comparison between the mathematical model of different particle size mineral mixtures optimized flotation and the actual flotation test results in the laboratory

Fig. 8 illustrates that the carrier effect correction of different particle size mineral mixtures flotation mathematic model may improve the reliability of the prediction, but the correction with the gap being big before 1.0min. Therefore, the different particle size mineral mixtures were

further modified, adding correction model derivation and laboratory actual average curve, to determine the error coefficient correction (Fig. 9). As indicated in Fig. 9, the difference between the laboratory practice and the mean curve is within the error range (2.5%), and the difference between the model derivation and the mean curve is also within the error range (2.5%). Therefore, after error correction, the correction coefficients of coarse particles are 1.64 ( $\alpha_1$ ), 1.25 ( $\alpha_2$ ), 0.89 ( $\alpha_3$ ), and 1.39 ( $\alpha_4$ ), respectively.

Therefore, the different particle size mineral mixtures flotation mathematical model corrected by two steps is  $y = 1.333t^3 - 11.222t^2 + 31.271t + 54.105$ . The change in particle size will generally affect the flotation of different particle-size mineral mixtures. Then the influence of the evolution of each coarse particle on the different particle size mineral mixtures flotation has been studied in depth (Fig. 10), to determine whether to optimize the granularity.

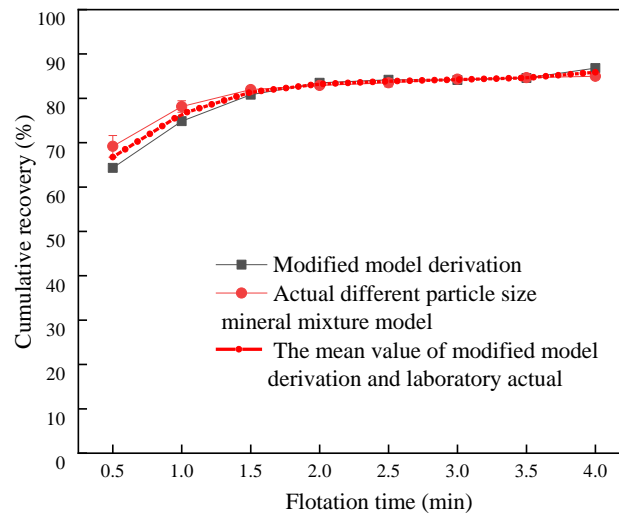


Fig. 9. The mean curve of modified model derivation and laboratory practice

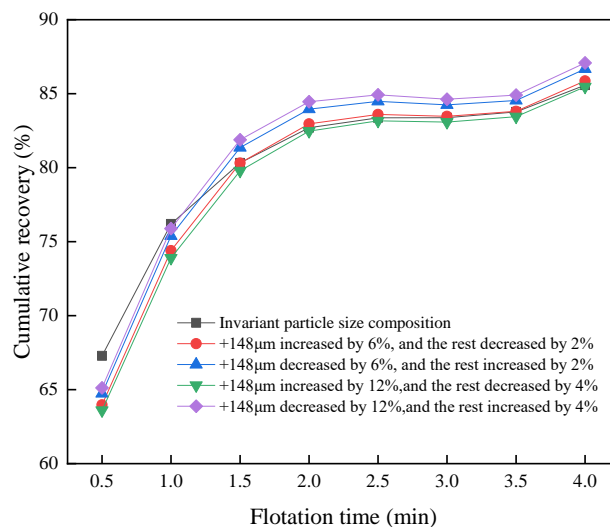


Fig. 10. Influence of each coarse particle composition on different particle size mineral mixtures flotation

As can be seen from Fig. 10, when the size +148 $\mu\text{m}$  increases by 6% (24.4% to 30.4%), the size of the rest decreases by 2%. When +148 $\mu\text{m}$  grain size increased by 12% (24.4% to 36.4%), the remaining grain size decreased by 4%. When +148 $\mu\text{m}$  grain size decreased by 6% (24.4% to 18.4%), the remaining grain size increased by 2%. When the size of +148 $\mu\text{m}$  decreases by 12% (24.4% to 12.4%), the size increases by 4%. From Fig. 10, the size composition changes, and the movement amplitude is small. That is, it

has little impact on the flotation of different particle-size mineral mixtures, and there is no need to optimize the size.

As demonstrated in Fig. 11, the prediction reliability of the two-step optimized different particle size mineral mixtures flotation mathematical model is greatly improved, which can accurately predict the flotation process index at any time in the flotation process.

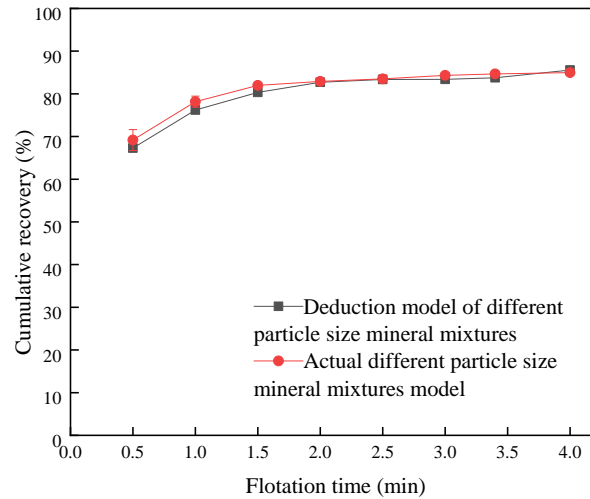


Fig. 11. Comparison between the optimized mathematical model of different particle-size mineral mixtures and the actual flotation test results in the laboratory

#### 4. Conclusion

This paper mainly investigates the effect of the particle size composition of molybdenite on its flotation kinetic model. Optical microscope observations and particle size analysis were used to identify the reasons for the decrease in accuracy of the flotation kinetic model due to changes in the composition of molybdenite particle size. The optimization method of the flotation kinetic model based on the particle size effect was innovatively proposed, which was not affected by the particle size effect. This work could also provide a theoretical basis for the development of flotation kinetic models for complex and variable conditions. The major conclusions can be drawn from the consequences as follows:

(1) The flotation rate increases first and then decreases with the flotation size increasing. The flotation rate of different particle-size mineral mixtures is better than others. The accuracy of the flotation mathematical model for different sizes is high. In contrast, the accuracy of the flotation mathematical model for the different particle size mineral mixtures is low.

(2) The autogenous carrier of the molybdenite was confirmed by optical microscope observations and particle size analysis. That is the reason for the decrease in the accuracy of the flotation kinetic model.

(3) The optimized different particle size mineral mixtures flotation mathematical model:  $y = 2.70t^3 - 18.78t^2 + 44t + 50.13$ , the reliability of its prediction is greatly improved. Additionally, it can accurately predict the flotation process index at any time in the flotation process.

#### Acknowledgments

This work was partially supported by the National Natural Science Foundation of China (Grant No. 52274271), the Natural Science Basic Research Plan in Shaanxi Province of China (No. 2022JM-284 and 2021JQ-507), the National Natural Science Foundation of China (Grant No. 52074206), the National Natural Science Foundation of China (Grant No. 51904222).

#### References

ABKHOSHK, E., KOR, M., REZAI, B., 2010. A study on the effect of particle size on coal flotation kinetics using fuzzy logic. *Expert Syst. Appl.* 37(7), 5201-5207.

- BU, X. N., XIE, G. Y., PENG, Y. L., 2017. *Interaction of fine, medium, and coarse particles in coal fines flotation*. Energy Sources Part A-Recovery Utilization and Environmental Effects. 39(12), 1276-1282.
- CHENG, G., LIU, J. T., CAO, Y. J., WANG, Y. T., LI, S. L., YUAN, C., 2013. *Comparison of the Flotation Performance between Wide and Narrow Particle Size Ranges of Coal*. Int. J. Coal. Prep. Util. 33(6), 290-299.
- FENG, Q. C., YANG, W. H., WEN, S. M., WANG, H., ZHAO, W. J., HAN, G., 2022. *Flotation of copper oxide minerals: A review*. Int. J. Min. Sci. Technol. <https://doi.org/10.1016/j.ijmst.2022.09.011>.
- GHARAI, M., VENUGOPAL, R., 2016. *Modeling of Flotation Process-An Overview of Different Approaches*. Miner. Process. Extr. Metall. Rev. 37(2), 120-133. <https://doi.org/10.1080/08827508.2015.1115991>.
- HUANG, G., XU, H. X., MA, L. Q., WU, L., 2018. *Improving Coal Flotation by Classified Conditioning*. Int. J. Coal. Prep. Util. 38(7), 361-373.
- HUANG, X., ZHANG, S., LIN, X. C., WANG, Y. G., XU, M., 2013. *Deoxygenation effect on hydrophilicity changes of Shengli lignite during pressurized pyrolysis at low temperature*. Journal of Fuel Chemistry and Technology. 41(12), 1409-1414.
- JOVICA, S., SANJA, M., 2018. *The effect of particle size on coal flotation kinetics: A review*. Physicochem. Probl. Miner. Process. 54(4), 1172-1190.
- LUO, C., HE, Y. Q., BU, X. N., XIE, W. N., WANG, H. F., WANG, S., 2015. *Improvement of Classical Dynamic Model for Flotation of Narrow Particle slime*. Journal of China University of Mining and Technology. 44(3), 477-482. <https://doi.org/10.13247/j.cnki.jcmt.000332>. (in Chinese).
- LIU, S. N., 2008. *57% molybdenum concentrate technology research and practice*. Non-ferrous Metals (Mineral Processing). (4), 6-9, 14 (in Chinese).
- LI, D., YIN, W. Z., LIU, Q., CAO, S. H., SUN, Q. Y., ZHAO, C., YAO, J., 2017. *Interactions between fine and coarse hematite particles in aqueous suspension and their implications for flotation*. Miner. Eng. 114, 74-81.
- LIU, A., FAN, M. Q., FAN, P. P., 2014. *Interaction mechanism of miscible DDA-Kerosene and fine quartz and its effect on the reverse flotation of magnetic separation concentrate*. Miner. Eng. 65(15), 41-50.
- NI, C., XIE, G. Y., JIN, M. G., PENG, Y. L., XIA, W. C., 2016. *The difference in flotation kinetics of various size fractions of bituminous coal between rougher and cleaner flotation processes*. Powder Technol. 292, 210-216.
- POLAT, M., POLAT, H., CHANDER, S., 2003. *Physical and chemical interactions in coal flotation*. Int. J. Miner. Process. 72(1-4), 199-213.
- QIU, G. Z., HU, Y. H., WANG, D. Z., 1994. *Study on flotation mechanism of Micro-fine hematite*. Nonferrous Metals. (04), 23-28. (in Chinese).
- RAHMAN, R. M., ATA, S., JAMESON, G. J., 2012. *The effect of flotation variables on the recovery of different particle size fractions in the froth and the pulp*. Int. J. Miner. Process. 106-109, 70-77.
- WANG, X. X., ZHOU, S. Q., BU, X. N., NI, C., XIE, G. Y., PENG, Y. L., 2020. *Investigation on interaction behavior between coarse and fine particles in the coal flotation using focused beam reflectance measurement (FBRM) and particle video microscope (PVM)*. Sep. Sci. Technol. 56(8), 1418-1430.
- XU, C. H., GUI, W. H., YANG, C. H., ZHU, H. Q., LIN, Y. Q., SHI, C., 2012. *Flotation process fault detection using output PDF of bubble size distribution*. Miner. Eng. 26, 5-12.
- XU, D., AMETOV, I., GRANO, S. R., 2013. *Quantifying rheological and fine particle attachment contributions to coarse particle recovery in flotation*. Miner. Eng. 39, 89-98.
- YANG, C. G., FENG, A. A., ZHU, J. B., YIN, J. Q., 2020. *Study on fine coal flotation based on the mathematical model*. Coal preparation Technology. (3), 12-15 (in Chinese).
- YUAN, L. X., LI, J., LI, Y., 2010. *Study on Dissemination Characteristics of Scaly Molybdenite and Prediction of Their Effects on Mineral Processing Results*. Mining and Metallurgical Engineering. 30(4), 50-53 (in Chinese).
- ZHANG, Z. J., LIU, J. T., XU, Z. Q., MA, L. Q., 2013. *Effects of clay and calcium ions on coal flotation*. Int. J. Min. Sci. Technol. 23(5), 689-692.
- ZHANG, X. L., HAN, Y. X., GAO, P., LI, Y. J., SUN, Y. S., 2019. *Effects of particle size and ferrichydroxo complex produced by different grinding media on the flotation kinetics of pyrite*. Powder Technol. 360, 1028-1036.
- ZHANG, X. F., HU, Y. H., SUN, W., XU, L. H., 2017. *The Effect of Polystyrene on the Carrier Flotation of Fine Smithsonite*. Minerals. 7(4). <https://doi.org/10.3390/min7040052>.